



Published in final edited form as:

Invest Radiol. 2013 July ; 48(7): 501–508. doi:10.1097/RLI.0b013e3182823591.

Renal Blood Oxygenation Level–Dependent Imaging:

Contribution of R2 to R2* Values

Pierre-Hugues Vivier, MD, PhD^{*,†}, Pippa Storey, PhD^{*}, Hersh Chandarana, MD^{*}, Akira Yamamoto, MD, PhD^{*}, Kristopher Tantillo, MD^{*}, Umer Khan, MD^{*}, Jeff L. Zhang, PhD^{*}, Eric E. Sigmund, PhD^{*}, Henry Rusinek, PhD^{*}, James S. Babb, PhD^{*}, Michael Bubenheim, PhD[‡], and Vivian S. Lee, MD, PhD, MBA^{*}

^{*}NYU Langone Medical Center, Department of Radiology, New York, NY

[†]Service de Radiologie INSERM U1096

[‡]Service de Biostatistiques, Rouen University Hospital, Rouen, Cedex, France

Abstract

Objectives—The aim of this study was to assess the impact of oral water and intravenous furosemide challenges on blood oxygenation level–dependent magnetic resonance imaging measurements in the kidney and to examine the contribution of R2 ($=1/T2$) to changes in R2* ($=1/T2^*$).

Materials and Methods—This Health Insurance Portability and Accountability Act–compliant study had institutional review board approval, and written informed consent was obtained from all subjects. Nine healthy volunteers were imaged at 3 T on 2 visits. During each visit, a baseline fasting magnetic resonance acquisition was followed by a diuretic challenge: oral water load for the first visit and furosemide for the second. R2* and R2 values in the renal cortex and medulla were measured using multiple gradient echo and multiple spin echo sequences, respectively, and R2' values were computed as $R2' = R2^* - R2$. Timed urinary output was also measured.

Results—Averaged across all subjects, the R2* response to furosemide was greater than to water and greater in the medulla than the cortex. The mean R2 responses exhibited the same trends but were uniformly smaller than the mean R2* responses. The peak changes in R2* and R2 appeared, on average, 10 to 14 minutes before peak urinary output. The median percentage contribution of R2 to R2* changes was 16% in the medulla after both challenges. In the cortex, the median contribution was 48% after water load and 58% after furosemide challenge.

Conclusions—The contributions of R2 to R2* changes after water load and furosemide challenge are not negligible, especially in the renal cortex. In routine clinical practice, R2* could be used alone as a rough surrogate for R2' in the medulla. However, in the cortex, both R2 and R2* should be measured to obtain accurate values of R2'.

Reprints: Pierre-Hugues Vivier, MD, PhD, Service d'imagerie pédiatrique et fœtale, INSERM U1096, CHU Charles Nicolle, 1 rue de Germont, 76031 Rouen Cedex, France. pierre-hugues.vivier@chu-rouen.fr.

Conflicts of interest: For the remaining authors, none were declared.

Keywords

kidney; MRI; BOLD imaging; R2*; R2; furosemide; water load

The renal medulla in mammals functions in a state of relative hypoxia. The steep corticomedullary gradient in the partial pressure of oxygen (P_{O_2}) results from the countercurrent blood flow through the medullary vasa recta and the high rate of oxygen consumption required for active reabsorption of sodium in the medullary thick ascending limb of the loop of Henle.¹ Medullary P_{O_2} has been measured in the range of 10 to 20 mm Hg,^{2,3} whereas mean venous blood P_{O_2} is about 40 mm Hg and cortical oxygenation is about 50 mm Hg. An increase in medullary hypoxia has been implicated in the development of acute renal failure⁴ and also plays a role in the pathophysiology of hypertension,⁵ diabetic nephropathy,⁶ and contrast-induced nephropathy after injection of iodinated contrast agents.⁷ Renal oxygenation has therefore been proposed as a useful marker of renal function in patients with various diseases.⁸

Blood oxygenation level–dependent (BOLD) magnetic resonance imaging (MRI) has the potential to assess intrarenal oxygenation noninvasively. Blood oxygenation level–dependent MRI exploits the paramagnetic properties of deoxyhemoglobin.⁹ Because the renal medulla is naturally hypoxic, it falls in the linear portion of the hemoglobin oxygen dissociation curve, making BOLD MRI a sensitive marker of P_{O_2} changes,¹⁰ especially at high field strengths. The presence of deoxyhemoglobin in the blood creates differences in magnetic susceptibility between the capillaries and surrounding extravascular tissue, causing dephasing among spins and increasing the transverse relaxation rate $R2^*$ ($=1/T2^*$).¹⁰ However, other factors such as B_0 shimming, the rate of renal blood flow, water content, and magnetic susceptibility effects unrelated to deoxyhemoglobin also affect $R2^*$ measurements. For this reason, most renal BOLD imaging has focused on changes in $R2^*$ ($R2^*$) in response to a pharmacologic or physiologic challenge. Since the landmark paper by Prasad et al,¹⁰ oral water load and intravenous (IV) furosemide injection have been the most commonly applied physiologic challenges. Both significantly increase medullary P_{O_2} . In the case of furosemide, the increase is caused by inhibition of the sodium pump, whereas for hydration, it results from the production of endogenous prostaglandin.¹¹

A further consideration in the use of $R2^*$ as a surrogate marker for tissue P_{O_2} is the fact that $R2^*$ is also affected by variations in $R2$ ($=1/T2$) because, for example, of changes in water content. Whereas $R2$ changes are considered negligible in brain applications, it has long been known that the kidney undergoes substantial changes in water content in response to physiological and pharmacological interventions.^{12,13} A measurement of $R2$ enables a more direct assessment of changes in oxygenation by correcting $R2^*$ for $R2$ changes:

$$R2' = R2^* - R2$$

The resulting parameter $R2'$ is directly sensitive to deoxyhemoglobin concentration, without being affected by the confounding effects of water content. Despite its importance, the impact of $R2$ has not been extensively examined. To our knowledge, only 1 small human

study at 1.5 T has simultaneously evaluated $R2^*$ and $R2$ after water load and furosemide.¹⁰ In that study, 24% of medullary $R2^*$ (-6.43 s^{-1}) after water load was found to be attributable to medullary $R2$ (-1.53 s^{-1}). Recent animal studies have also confirmed that $R2$ influences $R2^*$ values.^{14,15}

Higher field strength is advantageous for $R2^*$ imaging owing to the scaling of susceptibility effects with B_0 .¹⁶ We therefore chose to investigate renal $R2^*$, $R2$, and $R2'$ at 3 T. The goal of our study was to assess the impact of oral water and IV furosemide challenges on BOLD signals in the kidney and to examine the $R2$ contribution to $R2^*$ changes at 3 T.

MATERIALS AND METHODS

Study Design

Ten young healthy volunteers were enrolled. This Health Insurance Portability and Accountability Act-compliant study was approved by our institutional review board, and written informed consent was obtained from all subjects. The volunteers were imaged on 2 different visits with a time interval not exceeding 21 days. They were asked to fast overnight, that is, consume no food or water for at least 10 hours. At each visit, baseline imaging was followed by a diuretic challenge: oral water load for the first visit and furosemide injection for the second. Subjects were asked to void before any diuretic challenge.

During the first visit, volunteers were asked to drink 20 mL of water per kilogram of body weight within 15 minutes to induce water diuresis. Magnetic resonance imaging resumed 45 minutes after the beginning of water load and continued for a period of at least 30 minutes (Fig. 1).

During the second visit, 20 mg of furosemide was injected intravenously over 10 seconds and flushed with 10 mL of saline. Magnetic resonance imaging resumed 5 minutes thereafter and continued for a period of at least 30 minutes.

Magnetic Resonance Imaging

Magnetic resonance imaging was performed at 3 T (Tim Trio; Siemens Medical Solutions, Erlangen, Germany). A multielement phased array coil was used in combination with spine coil elements in the patient table for signal reception. After scout images were acquired, $R2^*$ measurements were made using a 2-dimensional (2D) multiple gradient echo (mGRE) sequence with a water-selective excitation pulse (repetition time [TR]/echo time [TE]/flip angle/bandwidth [BW], 70 milliseconds/4.3–42.7 milliseconds/ 30° /300 Hz/pixel) to acquire 12 images with an echo spacing of 3.5 milliseconds. The acquisition was performed within a 15-second breath-hold. A single coronal slice was acquired in the long axis of both kidneys. The field of view was 420 mm \times 336 mm, with an acquisition matrix of 320 \times 272 and slice thickness of 7 mm.

$R2$ measurements were made using a 2D multiple spin echo (mSE) sequence, which produced 7 images with TE values in increments of 22 milliseconds. The parameters of this sequence were as follows: TR/TE/refocusing pulse flip angle/BW/parallel acquisition/turbo

factor, 700 milliseconds/22–153 milliseconds/180°/521 Hz/pixel/GRAPPA 2/4. The imaging plane and spatial resolution were matched to the mGRE sequence, and the acquisition was performed within a 22-second breath-hold.

To improve accuracy, the acquisitions were performed twice for each time point, with a free breathing interval of at least 30 seconds between them to avoid an induced hypoxia. All measurements represent the average of the 2 acquisitions.

To measure urine output during both challenges, multislice axial 2D T2-weighted (T2W) fast spin echo acquisitions covering the entire bladder were performed between each set of renal mGRE and mSE acquisitions (TR/TE/refocusing pulse flip angle/echo train length/BW/field of view/matrix/slice thickness, 5700 milliseconds/91 milliseconds/180°/11/210 Hz/pixel/280 × 400/162 × 256/3 mm).

Two baseline measurements were performed at each visit to assess repeatability. Multiple gradient echo and mSE sequences were each run twice (baseline 1) and then the volunteer was taken out of the magnet. After 5 minutes, the subject returned into the magnet and the same acquisitions (baseline 2) were repeated with a completely new calibration. In total, 4 mGRE and 4 mSE acquisitions were performed before any diuretic challenge each day.

Over the 30-minute period after the diuretic challenge, 4 or 5 time points were acquired, where each time point consisted of 2 mGRE acquisitions, 2 mSE acquisitions, and 2 acquisitions over the bladder bracketing the other 4 acquisitions to measure urinary output (Fig. 1).

Each time point therefore consisted of 6 acquisitions with a total duration of 5 to 7 minutes. The volunteers were allowed to get out of the scanner at any time if they felt a need to void. After voiding, they were returned to the scanner, and the study was resumed.

Data Analysis

Images were analyzed offline using customized software routines in Matlab (The MathWorks, Inc, Natick, MA). R2 and R2* maps were generated by fitting the intensity data in each pixel as a function of TE to a monoexponential decay using a nonlinear least-squares Levenberg-Marquardt algorithm. In cases of rapid signal decay, the data were truncated by ignoring samples with intensity below twice the noise level.¹⁷

Two independent readers (with 12 years and 1 year of experience in abdominal imaging respectively) processed all data. Observers drew regions of interest (ROIs) over the left and right cortex and medulla on anatomic images (ie, images with short TE), where corticomedullary contrast was greatest. The corresponding R2* and R2 maps were displayed next to the anatomic images (Fig. 2). The observers were asked to avoid any susceptibility artifacts from bowel gas. Because each acquisition was performed during a separate breath-hold, ROIs could not be copied from one acquisition to another but were instead drawn independently on each set of images.

The $R2^*$ and $R2$ values of each pixel within each ROI were averaged to obtain a single representative mean value of $R2^*$ and $R2$ per subject for each region (ie, medulla or cortex) and each time point.

The observers were blinded to their measured values, which were automatically stored in an electronic file. $R2'$ values were calculated using the equation: where $R2^*$, $R2$, and $R2'$ were expressed in s^{-1} . $R2^*$, $R2$, and $R2'$ were defined as the changes (postdiuretic challenge – baseline) in $R2^*$, $R2$, and $R2'$ respectively.

$$R2' = R2^* - R2$$

Because all 3 $R2^*$, $R2$, and $R2'$ values are expected to decrease after a diuretic challenge, we computed the contribution of $R2$ to $R2^*$ for each time point as follows:

$$(\Delta R2 / \Delta R2^*) \times 100\%$$

To measure the rate of urine output during the diuretic challenges, 1 observer segmented the bladder areas on the T2W images with a validated semiautomatic segmentation tool¹⁸ and calculated bladder volumes using a modified Simpson rule. The rate of urine output was calculated from the bladder volumes as follows: where t_j and t_{j+1} are successive time points.

$$\text{Urine output} = (\text{Volume}(t_{i+1}) - \text{Volume}(t_i)) / (t_{i+1} - t_i)$$

Statistical Analysis

Paired-sample t tests were used to assess the differences in the following:

- Peak $R2^*$, $R2$, and $R2'$ responses to water load and furosemide;
- Time of peak $R2^*$ and $R2$ response in the cortex and medulla;
- Time of peak $R2^*$ and $R2$ response for each challenge;
- Peak urinary outputs after both challenges; and
- Time of peak urinary outputs for both challenges.

To assess whether there were systematic differences across baseline scans on the same day (with independent calibration), on different days, or according to different observers, paired-sample t tests were also used to evaluate differences in $R2$, $R2^*$, or $R2'$ values between the following:

- The 2 baseline scans on the same day. The data for each baseline scan of a given subject on a given day were represented as an average over both observers and both acquisitions.
- Two different days. For each day, the data for each subject were represented as an average over both observers and both measurements.

- Observers. For each observer, the data for each subject were represented as an average over all measurements from both baseline scans and both days.

To further assess measurement variability, the root mean square (RMS) of the differences was calculated. This metric incorporates both random variation and any systematic differences. We also computed the mean difference (bias) and standard deviation of the differences (SDD) based on the Bland-Altman method.

A linear regression analysis was performed to correlate peak $R2^*$, $R2$, and $R2'$ values with peak urinary output.

All reported P values are 2 sided, and statistical significance is defined as $P < 0.05$. SAS 9.0 (SAS Institute, Cary, NC) and Excel 2003 (Microsoft, Redmond, WA) were used for all statistical computations.

RESULTS

All 10 subjects successfully completed the imaging protocol. All had difficulty drinking the full amount of water but managed to do so, and all experienced some discomfort immediately after the oral water load.

For 1 volunteer, severe susceptibility artifacts on all $R2^*$ maps were noted, related to the presence of air in colonic flexures that prevented any measurements for either kidney. Data for this volunteer were excluded from the analysis. Hence, 9 individuals, including 5 men and 4 women, were analyzed. The mean age was 25.9 years (age range, 22–32 years).

A representative plot of changes in $R2^*$ and $R2$ in response to water and furosemide challenge over time is shown in Figure 3.

Peak urinary output during the study was consistently greater after furosemide injection (average peak output, 21.0 mL/min; range, 14–31 mL/min) than after water load (average peak output, 12.4 mL/min; range, 9.4–15.6 mL/min) ($P < 5 \times 10^{-4}$). The time of peak urine output was consistently earlier with furosemide (mean, 21.9 minutes after injection) compared with water load (mean, 69 minutes after the start of hydration) (Table 1).

$R2^*$ and $R2$ exhibited no significant difference in the time taken to reach maximum decrease (Table 1). The renal medulla and cortex showed the same kinetic pattern in response to hydration. After furosemide injection, however, the maximum decrease in $R2^*$ appeared significantly earlier (by 8.9 minutes; $P < 0.01$) in the medulla than in the cortex.

The results for $R2^*$, $R2$, and $R2'$ are shown in Table 2 and displayed graphically in Figure 4. $R2^*$, $R2$, and $R2'$ all decreased significantly after water load and furosemide injection. The changes were also significantly greater with furosemide than with water load in the medulla, although not in the cortex. The responses to water load exhibited more variability among subjects than the responses to furosemide did; in particular, 2 subjects showed no decrease in medullary $R2^*$ after water load ($R2^* = 0.47$ and 1.34).

The relative contribution of medullary R_2 to R_2^* with diuretic challenges (Fig. 5) was small but significant (with a median value of 16% for both water load and furosemide). This implies that medullary R_2^* was predominantly explained by R_2' (84%). In contrast, the median contribution of R_2 to cortical R_2^* was substantial (48% for water load and 58% for furosemide).

Mean R_2 , R_2^* , and R_2' baseline values over all subjects showed no systematic difference between the 2 visits. However, there was a slight systematic difference between the first and second baseline measurements in the cortex on the same day (Table 3).

The variability of the R_2 , R_2^* , and R_2' measurements on the same day and on different days is expressed by the RMS of the differences (displayed in Table 3). Measurements of R_2 were substantially less variable than R_2^* and R_2' , and measurements on the same day were less variable than measurements on different days.

Between the 2 observers, the baseline measures showed systematic differences in the cortex but not in the medulla (Table 3). The variability in medullary R_2^* estimates between observers was nevertheless substantial, with an RMS difference of 1.96 s^{-1} .

No significant correlation was found between peak R_2^* , R_2 , and R_2' values and peak urinary output.

DISCUSSION

This study is the first to assess changes in both R_2^* and R_2 in normal human kidney at 3 T after furosemide and water hydration challenges. We observed that R_2^* decreased significantly for both challenges, and a substantial component of the R_2^* changes were caused by reductions in R_2 , likely resulting from increased water content. Because fluid management is 1 of the primary functions of the kidney, it is not surprising that changes in R_2^* reflect changes not only in R_2' but also in R_2 . We showed that 16% of the median medullary R_2^* was explained by R_2 for both water load and furosemide. In the cortex, this percentage was much higher; R_2 comprised 48% of R_2^* after oral water load and 58% after furosemide injection (Fig. 5). Thus, using R_2^* as a surrogate for R_2' could introduce substantial errors in estimating cortical R_2' and a slight overestimation of the medullary R_2' in response to furosemide or hydration.

The R_2^* , R_2 , and R_2' responses to both diuretic challenges were all statistically significant, both in the cortex and medulla. This suggests that, over the healthy young adult population, furosemide and water load both have a real effect on tissue oxygenation and water content throughout the kidney. However, to assess the confidence with which responses can be evaluated in individual subjects, it is important to consider the uncertainty of the measurements. The relevant measure of uncertainty in this case is same-day variability, which can be estimated from the RMS differences given in Table 3. For example, the uncertainty in medullary R_2^* was about 1.44 s^{-1} . By comparison, the mean response to furosemide was $R_2^* = -8.40 \text{ s}^{-1}$, which is several times greater than this uncertainty. This suggests that the medullary R_2^* responses to furosemide measured in individual subjects may be treated with a fairly high degree of confidence. By contrast, the mean medullary R_2^*

response to water load was $R2^* = -3.79 \text{ s}^{-1}$, which is only about 2.6 times greater than the measurement uncertainty. This suggests that the relative medullary $R2^*$ responses of individual subjects should be regarded with slightly less confidence. The cortical $R2^*$ responses were similarly about twice the measurement uncertainty, suggesting moderate caution in comparing among individual subjects. $R2$ exhibited smaller responses than $R2^*$ but could be measured with greater accuracy. Thus, the measured $R2$ responses, corresponding to the main focus of our study, can be treated with a fairly high degree of confidence. Regarding $R2'$, the mean medullary response to furosemide was several times greater than measurement uncertainty, suggesting high confidence in the values for individual subjects. The medullary $R2'$ response to water load was only about twice the measurement uncertainty, suggesting moderate confidence, and the cortical $R2'$ responses were of the same order as measurement uncertainty, suggesting low confidence.

Most renal BOLD imaging studies for clinical applications have focused on medullary $R2^*$ measurements^{6,19,20} because the medulla is particularly prone to ischemia and to acute (and chronic) tubular necrosis. However, the renal cortex can be affected by other ischemic pathologies such as cortical necrosis and may benefit from noninvasive BOLD measurements. In this case, $R2^*$ is not an adequate surrogate for $R2'$, and adding an $R2$ measurement appears to be important for accurate estimation of $R2'$.

The increased water content, suggested by the $R2$ changes, may be explained as follows. Water load is responsible for endogenous prostaglandin production (PGE₂), which generates vasodilatory effects and a reduction in Na-K-ATPase activity in the thick ascending limb of the loop of Henle.^{21,22} Furosemide selectively inhibits the Na⁺-K⁺-ATPase pump in the thick ascending limb. Both challenges increase water flow in the ascending limb (located in medulla and cortex), as well as downstream in the distal convoluted tubules located in the cortex, and further distally in the collecting ducts (located partially in the cortex but mainly in the medulla). It is known that diuretics produce an enlargement of the kidney,^{23–28} which is associated with an increase in water content in both the cortex and medulla²⁹ and a reduction in $R2$.¹⁴ The observed $R2$ decrease in this study after both water load and furosemide in both cortex and medulla is thus likely related to an increase in water content.^{14,29} This explanation is corroborated by the observation that furosemide produced a larger medullary $R2$ response than water load did and was also associated with greater urine output. Cortical $R2$ decrease was also greater after furosemide than after water load, although the difference was not statistically significant (Fig. 4).

In agreement with previous reports, the $R2^*$ response to water load exhibited substantial variation among subjects, with some volunteers showing no significant change.^{20,30} Furosemide injection, by contrast, yielded more consistent reductions in $R2^*$ during the first minutes after the IV injection, and the medullary responses were, on average, twice as high as those produced by water load (Table 2 and Fig. 4).

We observed a small but significant decrease in cortical $R2^*$ after both hydration (-1.28 s^{-1}) and furosemide (-1.84 s^{-1}). There is some inconsistency in the literature concerning the cortical response to water load. Tumkur et al³¹ observed a similar reduction in cortical $R2^*$ (-1.0 s^{-1}) after water load at 3 T but reported it as insignificant, perhaps because of a lack of

statistical power ($n = 5$). In contrast, the seminal study by Prasad and Epstein²⁰ in young subjects at 1.5 T yielded a significant cortical $R2^*$ response to water load (-1.1 s^{-1}), although this finding was not confirmed in later studies.^{30,32} These inconsistencies in the literature may be caused, in part, by the difficulty of measuring $R2^*$ with sufficient precision, as suggested by our reproducibility data (Table 3). Our results suggest furthermore that the changes in cortical $R2^*$ after water load and furosemide are largely (although not wholly) attributable to changes in $R2$. This follows from our observation of significant changes in both $R2$ and $R2'$ (Table 2).

Furosemide injection has several features that favor it over oral water load for clinical BOLD imaging. Subject tolerance was superior in the sense that none of the volunteers experienced discomfort after furosemide injection, whereas all did so after oral water load. Furosemide injection provided a significantly higher peak urinary output than oral hydration did ($P < 5 \times 10^{-4}$), although both challenges exceeded the desired urinary output of 5 mL/min for BOLD imaging after a diuretic challenge.^{30,31} Furosemide also elicited a larger, more rapid, and more consistent renal response than did hydration, with a change in medullary $R2^*$ that was several times higher than the measurement uncertainty. Nevertheless, we acknowledge that where the objective is to evaluate prostaglandin production or endothelial function, hydration may be preferable over furosemide. Our study, combining measurements of $R2^*$ and $R2$ with calculations of urinary output, showed for the first time that the peak $R2^*$ and $R2$ responses preceded peak urinary output by an average of 10 to 14 minutes (Table 1). This new finding demonstrates that metabolic changes precede the diuretic response for both furosemide and water load. Our results showing peak urinary output at 21.9 minutes after furosemide injection were in line with published values.^{33,34} This time shift may plausibly explain the absence of significant correlation between peak urinary output and peak $R2^*$, $R2$, and $R2'$ values.

Our mean baseline medullary $R2^*$ value of 28.08 s^{-1} at 3 T is in close agreement with published data, namely, 26.4 to 30.3 s^{-1} with a comparable multiecho approach.^{16,31} To our knowledge, there are no published medullary and cortical $R2$ values based on a multiecho approach in vivo. Our values of 8.43 and 9.77 s^{-1} , respectively, were slightly lower than reported values based on single-echo approach with varying TEs at 3 T,³⁵ namely, 12.3 and 13.2 s^{-1} , respectively. This discrepancy is not surprising given the difference in acquisition technique. It is worth noting that there is no reference method for measuring $R2$. Multiecho approaches may slightly underestimate $R2$ values because of the contribution from stimulated echoes in the presence of imperfect refocusing pulses. Because stimulated echoes involve storage of magnetization on the longitudinal axis, their effect is to introduce a T1 component into the signal decay. Because T1 is always longer than T2, the resulting decay rate is slightly reduced. On the other hand, a single-echo approach with varying TEs tends to overestimate $R2$ values because of the effects of diffusion. Because the delay between the excitation and refocusing pulses increases for longer TE, the spins have more time over which to diffuse, resulting in greater dephasing. Thus, a single-echo approach tends to give higher $R2$ values than a multiecho technique does.

Small but significant systematic differences (or bias) in baseline cortical $R2^*$ and $R2$ values were observed between the first and second baseline scans on the same day (Table 3). This is

difficult to explain in terms of any real physiological changes or magnetic resonance calibration, as there were no significant systematic differences between baseline medullary values on the same day or between cortical and medullary values on different days. Further studies will be needed to determine whether this finding is reproducible or whether it is simply a type 1 statistical error.

Our study has several limitations. In 1 subject, we were unable to use the BOLD data because of bowel gas artifacts. In addition, our reproducibility analysis showed that $R2^*$ values had a relatively poor precision despite averaging over 2 acquisitions per time point and despite making the ROIs as large as possible without incurring partial volume effects (Fig. 2). The precision could possibly be improved by imaging multiple 2D slices to cover the entire kidney or by using a 3D acquisition. However, multiple 2D slices would take several breath-holds to image and 3D acquisitions usually have a lower spatial resolution than 2D acquisitions for a similar breath-hold duration.¹⁶ An alternative might be to perform a histogram analysis to exclude extreme values.³⁶ The interobserver variability in our results can be explained by the inherent subjectivity involved in manual segmentation and might be avoided by application of an automated compartmental analysis, which has been shown to provide reproducible and valid results with BOLD imaging.³⁷

We conclude that furosemide is a better diuretic challenge than oral water load because it is better tolerated, takes effect more quickly, and produces a larger $R2^*$ response in both the cortex and medulla. Using $R2^*$ as a surrogate for renal $R2'$ ignores changes in $R2$ and yields inaccurate results, particularly in the cortex. To assess renal $R2'$, $R2$ measurements must be performed in addition to conventional $R2^*$ measurements.

Acknowledgments

Sources of funding: Pierre-Hugues Vivier received a Fulbright's grant and a grant (Médaille d'or des hôpitaux de Rouen) from Rouen University Hospital.

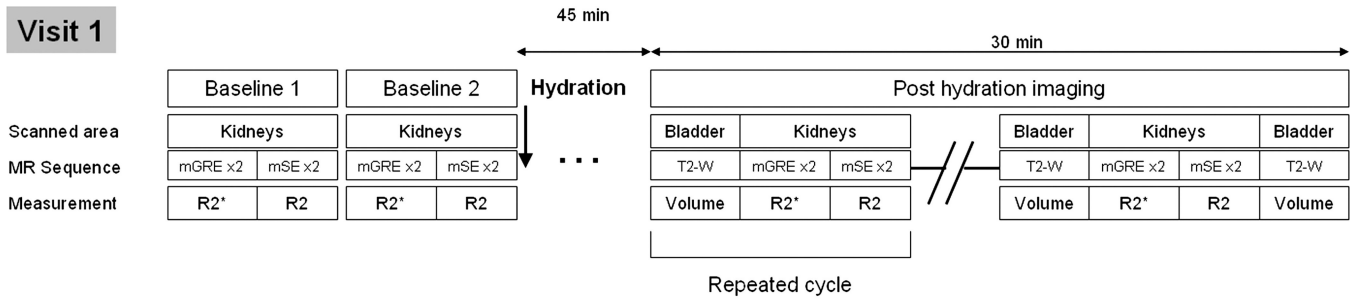
REFERENCES

1. Brezis M, Rosen SN, Epstein FH. The pathophysiological implications of medullary hypoxia. *Am J Kidney Dis.* 1989; 13:253–258. [PubMed: 2493191]
2. Brezis M, Heyman SN, Dinour D, et al. Role of nitric oxide in renal medullary oxygenation. Studies in isolated and intact rat kidneys. *J Clin Invest.* 1991; 88:390–395. [PubMed: 1864953]
3. Brezis M, Agmon Y, Epstein FH. Determinants of intrarenal oxygenation. I. Effects of diuretics. *Am J Physiol.* 1994; 267:F1059–F1062. [PubMed: 7810692]
4. Heyman SN, Brezis M, Reubinoff CA, et al. Acute renal failure with selective medullary injury in the rat. *J Clin Invest.* 1988; 82:401–412. [PubMed: 3403711]
5. Cowley AW Jr, Mattson DL, Lu S, et al. The renal medulla and hypertension. *Hypertension.* 1995; 25:663–673. [PubMed: 7721413]
6. Epstein FH, Veves A, Prasad PV. Effect of diabetes on renal medullary oxygenation during water diuresis. *Diabetes Care.* 2002; 25:575–578. [PubMed: 11874950]
7. Haneder S, Augustin J, Jost G, et al. Impact of iso- and low-osmolar iodinated contrast agents on BOLD and diffusion MRI in swine kidneys. *Invest Radiol.* 2012; 47:299–305. [PubMed: 22488508]
8. Gomez SI, Warner L, Haas JA, et al. Increased hypoxia and reduced renal tubular response to furosemide detected by BOLD magnetic resonance imaging in swine renovascular hypertension. *Am J Physiol Renal Physiol.* 2009; 297:F981–F986. [PubMed: 19640896]

9. Pauling L, Coryell CD. The magnetic properties and structure of hemoglobin, oxyhemoglobin and carbonmonoxyhemoglobin. *Proc Natl Acad Sci U S A*. 1936; 22:210–216. [PubMed: 16577697]
10. Prasad PV, Edelman RR, Epstein FH. Noninvasive evaluation of intrarenal oxygenation with BOLD MRI. *Circulation*. 1996; 94:3271–3275. [PubMed: 8989140]
11. Li LP, Halter S, Prasad PV. Blood oxygen level-dependent MR imaging of the kidneys. *Magn Reson Imaging Clin N Am*. 2008; 16:613–625. viii. [PubMed: 18926426]
12. Saikia TC. Composition of the renal cortex and medulla of rats during water diuresis and antidiuresis. *Q J Exp Physiol Cogn Med Sci*. 1965; 50:146–157. [PubMed: 14281638]
13. Trillaud H, Degreze P, Combe C, et al. Evaluation of intrarenal distribution of ultrasmall superparamagnetic iron oxide particles by magnetic resonance imaging and modification by furosemide and water restriction. *Invest Radiol*. 1994; 29:540–546. [PubMed: 8077093]
14. Storey P, Ji L, Li LP, et al. Sensitivity of USPIO-enhanced R2 imaging to dynamic blood volume changes in the rat kidney. *J Magn Reson Imaging*. 2011; 33:1091–1099. [PubMed: 21509866]
15. Yang X, Cao J, Wang X, et al. Evaluation of renal oxygenation in rat by using R2' at 3-T magnetic resonance: initial observation. *Acad Radiol*. 2008; 15:912–918. [PubMed: 18572128]
16. Tumkur S, Vu A, Li L, et al. Evaluation of intrarenal oxygenation at 3.0 T using 3-dimensional multiple gradient-recalled echo sequence. *Invest Radiol*. 2006; 41:181–184. [PubMed: 16428990]
17. Gudbjartsson H, Patz S. The Rician distribution of noisy MRI data. *Magn Reson Med*. 1995; 34:910–914. [PubMed: 8598820]
18. Mikheev A, Nevsky G, Govindan S, et al. Fully automatic segmentation of the brain from T1-weighted MRI using Bridge Burner algorithm. *J Magn Reson Imaging*. 2008; 27:1235–1241. [PubMed: 18504741]
19. dos Santos EA, Li LP, Ji L, et al. Early changes with diabetes in renal medullary hemodynamics as evaluated by fiberoptic probes and BOLD magnetic resonance imaging. *Invest Radiol*. 2007; 42:157–162. [PubMed: 17287645]
20. Prasad PV, Epstein FH. Changes in renal medullary PO₂ during water diuresis as evaluated by blood oxygenation level-dependent magnetic resonance imaging: effects of aging and cyclooxygenase inhibition. *Kidney Int*. 1999; 55:294–298. [PubMed: 9893139]
21. Jabs K, Zeidel ML, Silva P. Prostaglandin E2 inhibits Na⁺-K⁺-ATPase activity in the inner medullary collecting duct. *Am J Physiol*. 1989; 257:F424–F430. [PubMed: 2551187]
22. Silva P, Rosen S, Spokes K, et al. Influence of endogenous prostaglandins on mTAL injury. *J Am Soc Nephrol*. 1990; 1:808–814. [PubMed: 2133430]
23. Dorph S, Oigaard A. Renal distension in response to water-soluble contrast medium and various diuretics. *Scand J Urol Nephrol*. 1975; 9:114–118. [PubMed: 1145141]
24. Dorph S, Sovak M, Talner LB, et al. Why does kidney size change during I.V. urography? *Invest Radiol*. 1977; 12:246–250. [PubMed: 863628]
25. Finberg JP, Peart WS. Renal tubular flow dynamics during angiotensin diuresis in the rat. *Br J Pharmacol*. 1970; 39:357–372. [PubMed: 4316597]
26. Hegedus V, Faarup P, Norgaard T, et al. Volume changes in the rat renal cortex during urography. *Br J Radiol*. 1978; 51:793–798. [PubMed: 709020]
27. Omvik P Jr, Raeder M, Kiil F. Determinants of renal cortical volume. *Am J Physiol*. 1971; 221:1560–1567. [PubMed: 4330897]
28. Wolpert SM. Variation in kidney length during the intravenous pyelogram. *Br J Radiol*. 1965; 38:100–103. [PubMed: 14254050]
29. Pedersen M, Vajda Z, Stodkilde-Jorgensen H, et al. Furosemide increases water content in renal tissue. *Am J Physiol Renal Physiol*. 2007; 292:F1645–F1651. [PubMed: 17264309]
30. Li LP, Storey P, Pierchala L, et al. Evaluation of the reproducibility of intrarenal R2* and DeltaR2* measurements following administration of furosemide and during waterload. *J Magn Reson Imaging*. 2004; 19:610–616. [PubMed: 15112311]
31. Tumkur SM, Vu AT, Li LP, et al. Evaluation of intra-renal oxygenation during water diuresis: a time-resolved study using BOLD MRI. *Kidney Int*. 2006; 70:139–143. [PubMed: 16572109]
32. Zuo CS, Rofsky NM, Mahallati H, et al. Visualization and quantification of renal R2* changes during water diuresis. *J Magn Reson Imaging*. 2003; 17:676–682. [PubMed: 12766897]

33. Brown SC, Upsdell SM, O'Reilly PH. The importance of renal function in the interpretation of diuresis renography. *Br J Urol.* 1992; 69:121–125. [PubMed: 1537020]
34. Upsdell SM, Leeson SM, Brooman PJ, et al. Diuretic-induced urinary flow rates at varying clearances and their relevance to the performance and interpretation of diuresis renography. *Br J Urol.* 1988; 61:14–18. [PubMed: 3342295]
35. de Bazelaire CM, Duhamel GD, Rofsky NM, et al. MR imaging relaxation times of abdominal and pelvic tissues measured in vivo at 3.0 T: preliminary results. *Radiology.* 2004; 230:652–659. [PubMed: 14990831]
36. Rossi C, Artunc F, Martirosian P, et al. Histogram analysis of renal arterial spin labeling perfusion data reveals differences between volunteers and patients with mild chronic kidney disease. *Invest Radiol.* 2012; 47:490–496. [PubMed: 22766911]
37. Ebrahimi B, Gloviczki M, Woollard JR, et al. Compartmental analysis of renal BOLD MRI data: introduction and validation. *Invest Radiol.* 2012; 47:175–182. [PubMed: 22183077]

Visit 1



Visit 2

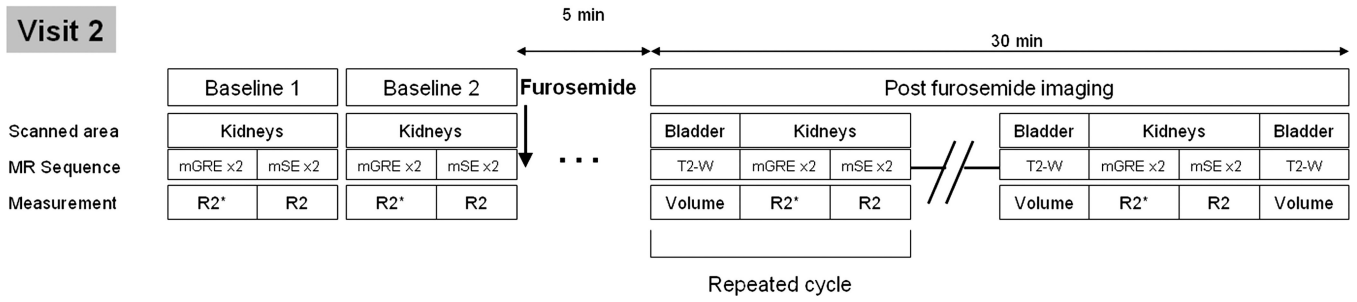


FIGURE 1. Study timeline. Each cycle of measurements (corresponding to 1 time point) was repeated in rapid succession over a period of at least 30 minutes after the diuretic challenges, for a total of 4 to 5 cycles. T2-W indicates T2W fast spin echo sequence.

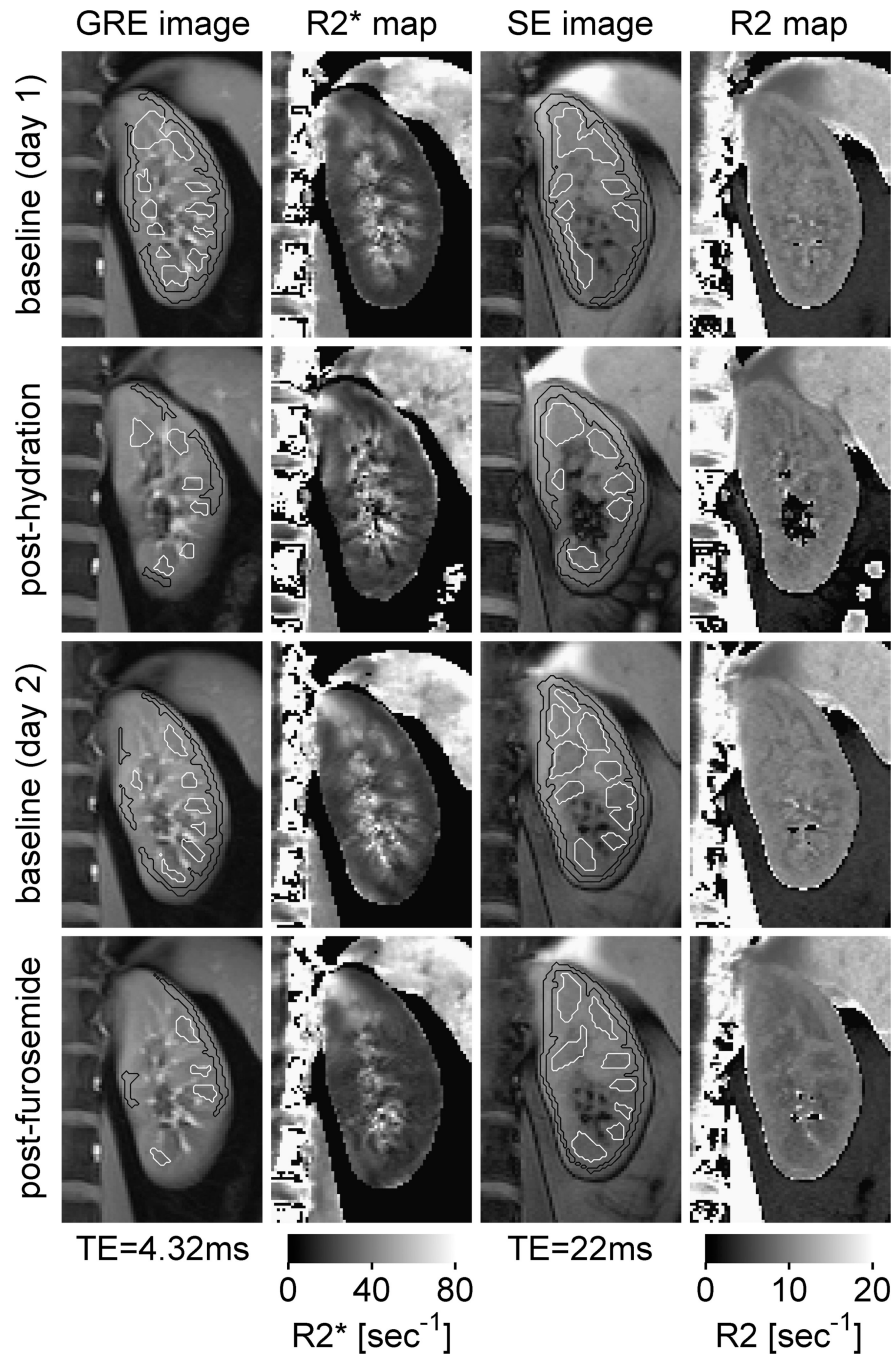


FIGURE 2.

Cortical and medullary ROIs drawn on T2* and T2 images with their corresponding R2* and R2 maps on cropped images over the left kidney. Note that the medullary R2* values decreased after water load and after furosemide as compared with the baseline states. SE indicates spin echo.

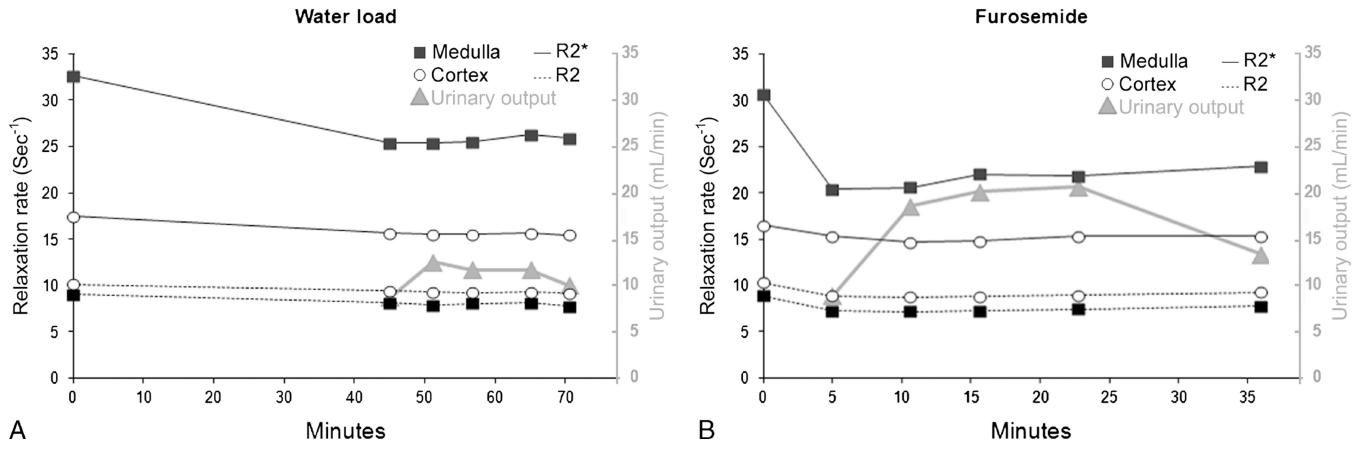


FIGURE 3. Representative changes in R2*, R2, and urinary output in response to water (A) and furosemide (B) challenge in 1 volunteer. Time 0 corresponds to the beginning of the diuretic challenge. The long time interval between the fifth and sixth measurements after furosemide injection was caused by the need to void.

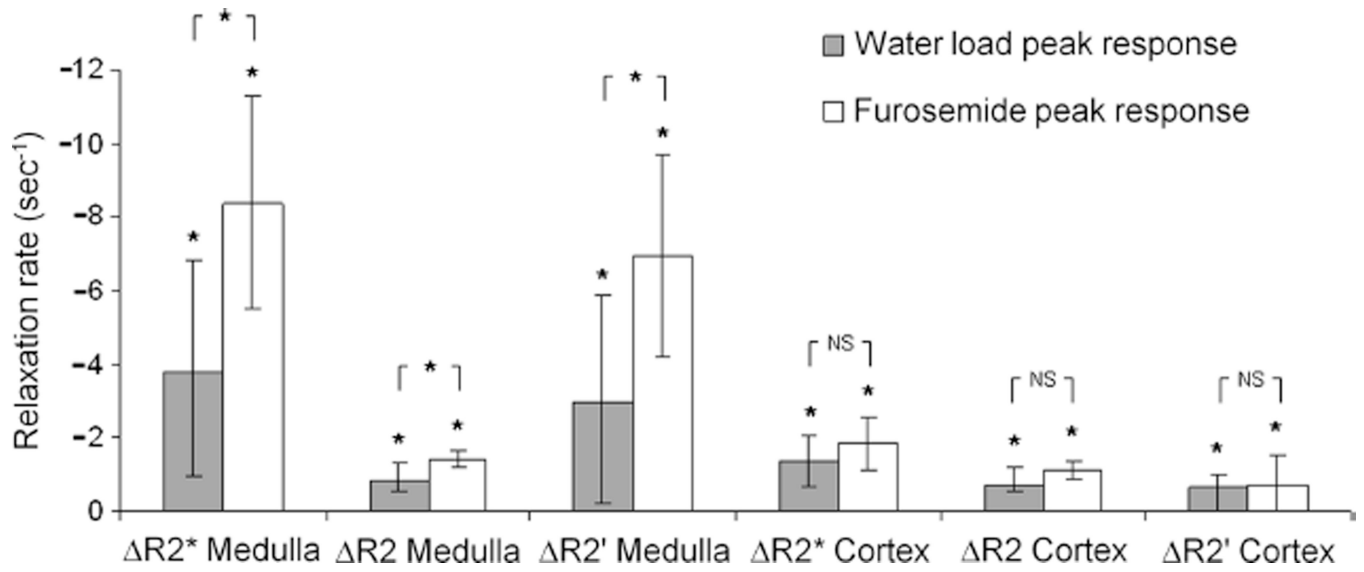


FIGURE 4. Peak $R2^*$, $R2$, and $R2'$ (postchallenge – prechallenge) after water load and furosemide in the cortex and in the medulla. *Significant. NS indicates nonsignificant.

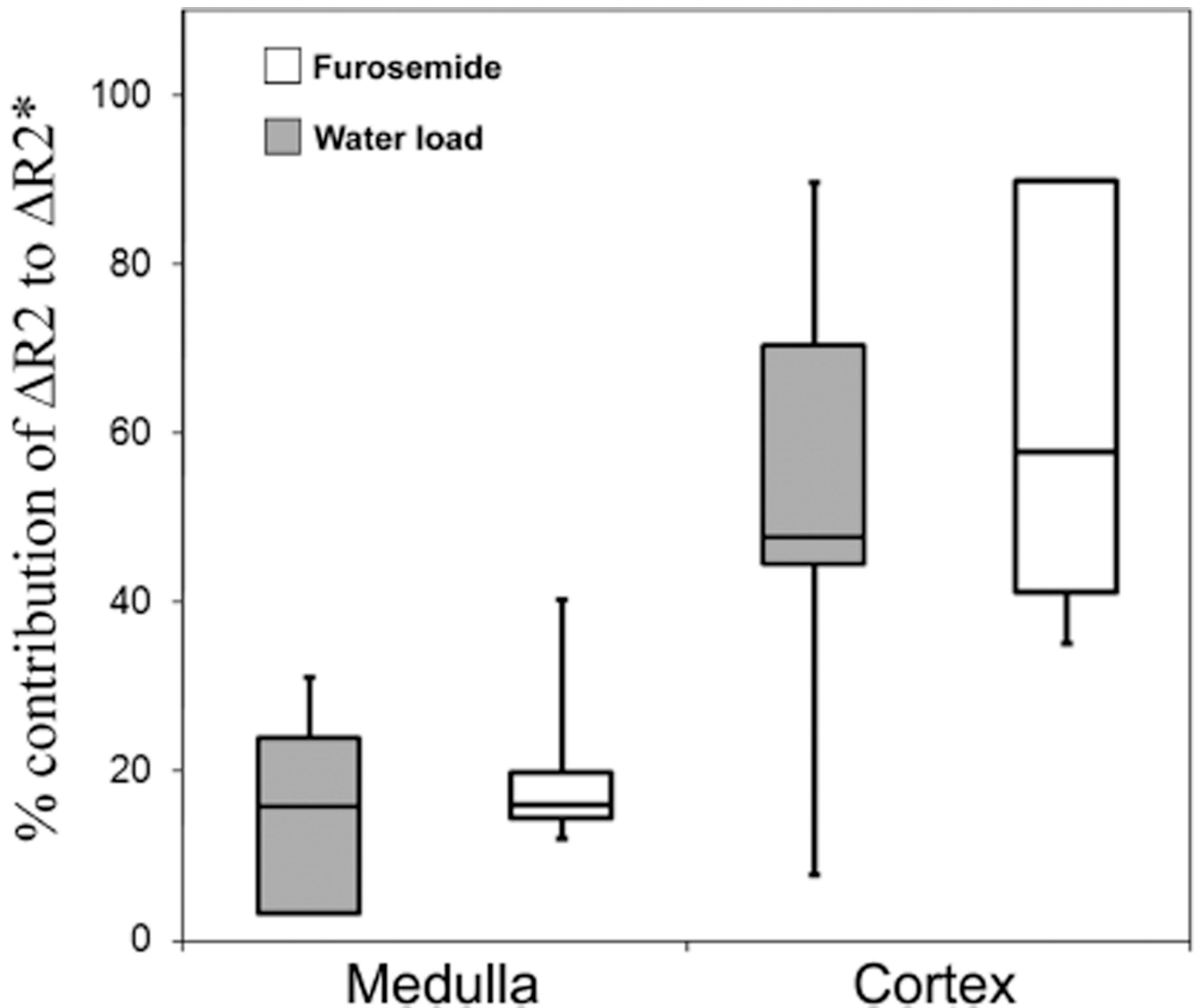


FIGURE 5.

Box-and-whisker plots displaying the relative contribution of changes in R2 to changes in R2* after furosemide and water load challenges. The median contribution of medullary R2 to medullary R2* was 16% after both challenges. The median contribution of cortical R2 to cortical R2* was 48% and 58% after water load and furosemide injection, respectively. Each box contains the middle 50% of the distribution (interquartile range), with the inner horizontal line corresponding to the median value. The ends of the tails correspond to the extreme values. The lower tail of the medullary response to water load and the upper tail of the cortical response to furosemide have been omitted because of outlying values for which percentage contribution makes no sense. The existence of these outlying values can be explained by the poor reproducibility of the R2* values.

TABLE 1

Times of Peak Urine Output and Peak R2 and R2* Response

	Time of Peak Urine Output, min	Medulla Cortex <i>P</i>	Time of Peak R2*, min	54.8 (45–66) 55.7 (45–66) 0.29	Time of Peak R2, min	55.7 (45–66) 55.7 (45–65) 0.5	<i>P</i>	Medulla Cortex	Time Shift Between Time of Peak Urine Output and	
									Peak R2*	Peak R2
Hydration	69 (57.6–77.7)	Medulla Cortex <i>P</i>	54.8 (45–66) 55.7 (45–66) 0.29	55.7 (45–66) 55.7 (45–65) 0.5	0.39 0.14	<10 ⁻³ <10 ⁻³	<10 ⁻³ <2 × 10 ⁻³			
Furosemide	21.9 (10.5–29.8)	Medulla Cortex <i>P</i>	7.6 (5–15) 16.4 (5–37) <0.01	11.2 (5–22) 10.7 (5–22) 0.38	0.06 0.09	<10 ⁻³ 0.13	<2 × 10 ⁻³ <10 ⁻³			

Mean times are provided, as well as minimum and maximum times (in parentheses). Times are in minutes, with the starting point corresponding to the beginning of the diuretic challenge.

R2* Values and Corresponding R2 and R2' Values Before and After Diuretic Challenges at Peak R2* Values

TABLE 2

	Pre-Water Load	Post-Water Load	P	Pre Furosemide	Post Furosemide	P
R2* Medulla	28.29 (23.01; 32.62)	24.49 (21.14; 29.45)	<6 × 10 ⁻³	27.87 (22.56; 32.23)	19.47 (16.45; 24.27)	<3 × 10 ⁻⁵
Cortex	17.25 (15.65; 18.54)	15.88 (14.82; 18.10)	<5 × 10 ⁻⁴	17.07 (15.70; 18.07)	15.23 (14.34; 16.17)	<7 × 10 ⁻⁵
R2 Medulla	8.44 (7.83; 9.05)	7.64 (6.45; 8.19)	<2 × 10 ⁻³	8.41 (7.74; 8.86)	6.97 (6.62; 7.44)	<2 × 10 ⁻⁷
Cortex	9.72 (9.14; 10.16)	8.99 (7.99; 9.69)	<2 × 10 ⁻³	9.82 (9.17; 10.46)	8.69 (8.13; 9.16)	<3 × 10 ⁻⁷
R2' Medulla	19.85 (15.18; 23.57)	16.86 (12.99; 21.89)	<0.02	19.46 (13.88; 23.74)	12.49 (9.76; 17.45)	<6 × 10 ⁻⁵
Cortex	7.53 (6.51; 8.66)	6.89 (6.03; 8.55)	<2 × 10 ⁻³	7.25 (6.13; 8.85)	6.54 (5.96; 7.30)	<0.04

Data are presented as mean (min; max).

Mean R2*, R2, and R2' decreased significantly after water load and furosemide injection for the medulla and cortex, most significantly after furosemide in the renal medulla.

TABLE 3

Differences in R2*, R2, and R2' Baseline Values Between Different Visits, Baselines, and Observers

Measure	Region	Day 1	Day 2	Mean Difference ± SDD	P	RMS Difference
R2*	Medulla	28.29 ± 3.05	27.87 ± 3.48	0.41 ± 1.94	0.540	1.87
	Cortex	17.25 ± 1.06	17.07 ± 1.10	0.18 ± 0.86	0.545	0.83
R2	Medulla	8.44 ± 0.42	8.41 ± 0.42	0.03 ± 0.15	0.585	0.14
	Cortex	9.72 ± 0.33	9.82 ± 0.48	-0.10 ± 0.32	0.368	0.32
R2'	Medulla	19.85 ± 2.61	19.46 ± 3.31	0.39 ± 1.93	0.564	1.86
	Cortex	7.53 ± 0.77	7.25 ± 1.02	0.28 ± 0.88	0.365	0.88

Measure	Region	Baseline 1	Baseline 2	Mean Difference ± SDD	P	RMS Difference
R2*	Medulla	27.86 ± 3.09	28.30 ± 3.06	-0.44 ± 1.45	0.216	1.44
	Cortex	17.40 ± 0.88	16.91 ± 0.96	0.49 ± 0.59	0.003	0.74
R2	Medulla	8.45 ± 0.32	8.40 ± 0.39	0.05 ± 0.13	0.108	0.13
	Cortex	9.85 ± 0.42	9.68 ± 0.39	0.17 ± 0.11	<6 × 10 ⁻⁶	0.20
R2'	Medulla	19.41 ± 2.99	19.90 ± 2.98	-0.49 ± 1.45	0.167	1.45
	Cortex	7.55 ± 0.85	7.23 ± 1.02	0.32 ± 0.60	0.037	0.65

Measure	Region	Observer 1	Observer 2	Mean Difference ± SDD	P	RMS Difference
R2*	Medulla	28.19 ± 3.30	27.97 ± 2.88	0.22 ± 2.07	0.755	1.96
	Cortex	16.83 ± 0.82	17.49 ± 0.82	-0.66 ± 0.45	0.002	0.78
R2	Medulla	8.29 ± 0.41	8.56 ± 0.38	-0.27 ± 0.36	0.052	0.43
	Cortex	9.82 ± 0.40	9.72 ± 0.36	0.10 ± 0.06	0.001	0.11
R2'	Medulla	19.90 ± 3.25	19.41 ± 2.75	0.49 ± 2.11	0.504	2.05
	Cortex	7.01 ± 0.82	7.77 ± 0.83	-0.75 ± 0.44	0.001	0.86

This provides a useful estimate of measurement uncertainty because it incorporates both the SDD and any bias between measurements (expressed by the mean difference). R2*, R2, and R2' values are expressed in s⁻¹.